Beni-Suef University Journal of Basic and Applied Sciences

RESEARCH

Open Access

Preparation of bee venom-loaded chitosan nanoparticles for treatment of streptozotocin-induced diabetes in male Sprague Dawley rats

Alyaa Farid[1*], Adham Mohamed[2], Ayten Ahmed[2], Farah Mehanny[2] and Gehan Safwat[2]

Abstract

Background Diabetes mellitus (DM) can be defined as an increase in the blood sugar level and a disturbance in protein, fat and carbohydrate metabolism. Bee venom (BV) is useful for treating and preventing diabetic rats' histological and biochemical problems. Although the medical advantages of BV have been identified, its safety has remained a substantial barrier for its application. Consequently, the goal of our work was to prepare bee venom-loaded chitosan (BV-CS) nanoparticles (NPs), which would then be physically characterized. This was followed by examining the effect of the synthetized BV-CS NPs on oxidation, inflammation and coagulation in vitro. In diabetic rats' model [induced by streptozotocin (STZ)], the produced BV-CS NPs were tested as an anti-diabetic medication.

Results In vivo testing on pancreatic tissue homogenates showed that BV-CS NPs have antioxidant and anti-inflammatory properties. The results showed that BV-CS NPs can be used as a safe and efficient therapy for diabetes. Up to a concentration of 250 µg/ml, the generated NPs demonstrated potential antioxidant, membrane stabilizing, and non-cytotoxic capabilities. Our findings indicated that the administration of BV-CS NPs significantly controlled blood glucose levels and metabolic abnormalities that accompanied diabetes induction.

Conclusions BV-CS NPs were successful in treating STZ-induced diabetes in rats, stimulated insulin secretion and were safe to be used in vivo.

Key points

1. BV-CS NPs demonstrated potential in vitro antioxidant and non-cytotoxic capabilities.
2. BV-CS NPs increased insulin secretion and decreased blood sugar level.
3. BV-CS NPs reduced oxidative stress and inflammation in vivo.

Keywords Bee venom, Chitosan, Diabetes mellitus, Cytokines

*Correspondence:
Alyaa Farid
alyaafarid@cu.edu.eg
Full list of author information is available at the end of the article

Graphical abstract

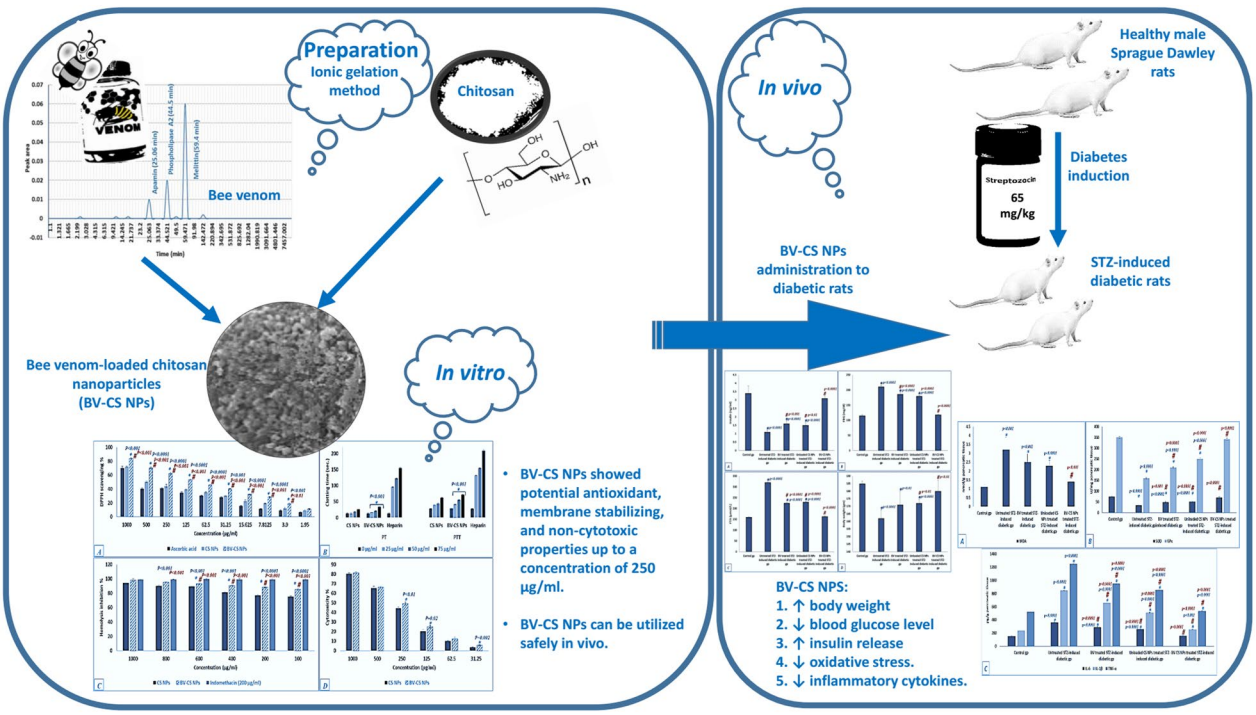

1 Background

According to Tan et al. [1], diabetes mellitus (DM) is among the ancient human diseases. It is a metabolic disorder that is, frequently, characterized by high levels of glucose in the blood that require ongoing checking and effective management. For the majority of individuals worldwide, DM is becoming more common in all nations, regardless of their economic level [2]. By the year 2049, over six million individuals are predicted to be diabetic, according to English and Lenters-Westra [3]. The development of novel treatment entities is greatly aided by the scientific and technical advancements since DM is a significant economic burden for many nations [4].

With the insulin discovery in the mid-1920s, significant progress has been achieved in the treatment of diabetes [5]. Anti-hyperglycemic medications, nowadays, focus on a number of pathophysiological processes, including insulin secretion, glucose uptake and glucose re-absorption [6]. Though insulin analogues are still an effective method for treating DM in its advanced stages, insulin administration is no longer utilized to treat DM in early stages. There are several recognized oral drugs that reduce elevated blood glucose levels in addition to insulin [7]. Most of these medications have negative side effects that make it necessary to replace them with natural alternatives [8]. Nowadays, many natural drugs have been assigned for the treatment of many diseases such as cancer (indole compounds), wounds (Aloe vera), colitis (taurine) and diabetes (indole alkaloids) [9–12]. Recently, the poisonous products of several species have received a lot of interest in the development of remedies for numerous disorders, including DM [13].

Bee venom (BV) has been used medicinally for between 3000 and 5000 years in China, as well as in ancient Egypt [14]. Apitox, the brand name for BV, is a mixture of several chemicals including enzymes like phospholipase A2 (accounts for 12% of BV) and hyaluronidase, in addition to other components (non-peptide) like dopamine [15]. BV, also, contains melittin (60% of BV), adolapin, apamin and mast cell degranulating peptides. BV has been utilized for treating chronic inflammatory diseases, in traditional medicine, because it has a variety of pharmacological actions [16]. Studies conducted in vivo and in vitro have investigated the pharmacotherapy of BV [17–19] like anti-tumor, anti-nociceptive, radioprotection [20], anti-toxic, anti-apoptotic, antioxidant [19], antibacterial, antiviral, anti-inflammatory [18, 19],

neuroprotection [18], anti-arthritic [17], painkilling potencies, anti-metastatic effects [21].

Hassan et al. [22] reported that BV may have medicinal and preventative benefits on the control of histological and biochemical abnormalities in diabetic rats. Khulan et al. [23] studied the effect of Mongolian BV in alloxan-induced diabetic rabbits and reported its hypoglycemic effect; they added that this result was due to the reduction in pancreatic β cells inflammation, enhancement of insulin production, and stimulation of glucose and lipid absorption in adipose tissue. Mousavi et al. [24] reported that BV boosted insulin production in diabetic rat's model to normal levels; and added that the two primary components of BV, melittin polypeptide and phospholipase A2, have been shown to increase insulin secretion. Studies indicated that extracellular calcium and calcium channels mediated the hypoglycemic effect of BV [25–28]. Ullah et al. [29] demonstrated that the severity of inflammatory response and the development of diabetes decreased after BV therapy in research on the development of insulin-dependent diabetes. According to Morgan and Montague [25], melittin stimulated insulin release from β cells ex vivo; which pointed to melittin as a promising option for more research.

Even though BV's medicinal benefits have been demonstrated, its safety remained a significant limiting factor for its use [29]. The side effects of BV varied from minor skin allergies that go away within a few days to hemolysis, nerve damage and severe anaphylactic reactions that can be fatal [30, 31]. Allergic reaction [32], chronic inflammation [33], administration times and concentration of BV [29] are possible explanations for these negative effects. It is widely known that in addition to causing inflammation, BV injections also produce discomfort [34]. According to Chen et al. [35], melittin (a major component of BV) injection under the skin generated tonic pain via the stimulation of primary nociceptor cells, either directly or indirectly. Because of BV's short plasma half-life and the difficulty in choosing a precise dosage, researchers and investigators have promoted and developed various options, like combining BV with polymers or loading it on nanoparticles (NPs) [36].

Chitosan (CS), which consists of N-acetylglucosamine and glucosamine units, has a semi-crystalline structure, anti-inflammatory, antioxidant [37], and antibacterial properties with no toxicity [38]. Because of CS well-known mucoadhesive properties and capacity to increase the passage of large molecules through the cell membranes, it is frequently utilized for NPs preparation [39]. It has been demonstrated that CS NPs have a strong capability for protein interaction. Also, the delivery of polypeptides like snake venom and toxoid of diphtheria or tetanus using CS NPs was being studied in great detail [40, 41]. Elnosary et al. [42] reported that CS's use in the nanoform as a BV carrier was made possible by its biocompatibility, biodegradability, and non-toxicity.

Therefore, our study aimed to load bee venom on chitosan nanoparticles (BV-CS NPs), followed by its physical characterization and examining its outcome on oxidation, hemolysis inhibition, coagulation and cells viability in vitro. BV-CS NPs were examined as an anti-diabetic drug in streptozotocin (STZ)-induced diabetic rats. This was accomplished by measuring animals' body weight; level of fasting blood glucose (FBG), insulin and fructosamine (FTA) in different experimental groups. The effect of BV-CS NPs on the reduction of oxidation and inflammation was determined, in vivo, in pancreatic tissue homogenates.

2 Materials and methods

2.1 Materials

CS (low molecular weight, 448,869), sodium tripolyphosphate (TPP, 238,503) and STZ (S0130) were obtained from Sigma Aldrich Co. USA. Dried BV powder (MBS348001) was obtained from MyBioSource, USA. BV was collected from *Apis mellifera*, has a pale yellow color and contains melittin (64.4%), phospholipase A2 (14.4%) and apamin (2.67%). BV was explored by high-performance liquid chromatography (HPLC) to confirm the major components.

2.2 Synthesis of BV-CS NPs

Nanoparticles were synthetized by the ionic gelation method by combining CS (cation) and TPP (anion) [42]. CS (1.5 mg/ml) was dissolved in aqueous acetic acid solution (49.5 ml H_2O + 0.5 ml acetic acid) and stirred for 120 min at room temperature. TPP (0.75 mg/ml) was dissolved in water (20 ml) and stirred at room temperature for 30 min. The TPP solution was added to the CS solution followed by mixing at room temperature for 60 min until the stabilization of CS NPs. BV, in varied concentrations (0.5–4 mg/ml), was mixed with TPP solution and then added to CS solution to create BV-CS NPs. Nanoparticles (CS NPs and BV-CS NPs) were freeze-dried and kept in the refrigerator.

2.3 Characterization of NPs

Using scanning electron microscope (SEM) and transmission electron microscope (TEM), the shape of produced BV-CS NPs was determined. Dynamic light scattering technique was used to assess the NPs hydrodynamic size; also, the surface charge (zeta potential) was measured by a zetasizer. Additionally, BV, CS, CS NPs

and BV-CS NPs were identified throughout the Fourier transform infrared (FTIR) spectra.

2.4 Assessment of the encapsulation efficiency (EE)%

The EE% was determined (indirectly) by measuring the amount of BV that was not encapsulated in the NPs. BV-CS NPs solution was filtered followed by centrifugation for 60 min at 12,000 rpm. The protein content (indicating free BV) was measured using the Bradford protein assay spectrophotometric technique at 595 nm after the supernatant was collected [43]. According to Gan et al. [44] description, encapsulation efficiency was determined using the next equation.

$$EE\% = \frac{\text{Original amount of BV - Free amount of BV in supernatant}}{\text{Original amount of BV}} \times 100$$

2.5 In vitro *release study*

NPs (10 mg) were suspended in 3 ml of PBS/0.1% Tween-80 buffers (release media) followed by incubation at 37 °C. Hundred microliters of eluted samples was removed from the solution and centrifuged (after 2, 4, 6, 8, 16, 24, 48 and 72 h of incubation); this volume was replaced with fresh buffer to prevent sink conditions. Protein content was estimated by using the Bradford technique.

2.6 *The antioxidant effect of NPs* in vitro *(DPPH scavenging effect)*

One ml of 1, 1-diphenyl-2-picryl hydrazyl (DPPH), in ethyl alcohol solution, was mixed with various concentrations of nanoparticles (1000, ……., 3.9 µg/ml) and incubated at room temperature for half an hour with continuous shaking [45]. The absorbance (A) was measured at 517 nm. The next equation was employed to determine the DPPH scavenging activity (S. Act.) %.

DPPH S. Act. % = [(A control − A sample)/A control] × 100, where the control was ascorbic acid.

2.7 *The anti-coagulation effect of NPs* in vitro

The anti-coagulant effect of BV-CS NPs was estimated by the determination of the clotting time using heparin (as a control) and reagents for measuring prothrombin time (PT) and partial thromboplastin time (PTT) [45]. Hundred microliters of NPs (25, 50, or 75 ug/ml) was mixed with rat plasma (900 ul) at 37 °C.

2.8 *The anti-inflammatory effect of NPs* in vitro *(membrane stabilization) assay*

Red blood cells (RBCs) were prepared from heparinized fresh rat blood. Three ml blood was centrifuged for 10 min at 2500 rpm followed by discarding the supernatant, and the pellet was dissolved in saline buffer (40% v/v) [45]. Different concentrations of BV-CS NPs (1000, ……. 100 µg/ml) were diluted in five ml of pure H_2O or five ml of saline solution. Nanoparticles solutions and indomethacin (control) were mixed with the generated erythrocytes' suspension, left for 60 min at 37 °C. The released hemoglobin was determined at 540 nm:

Hemolysis inhibition % = 1 − [(A sample in water − A sample in saline)/(A control − A sample in saline)] × 100.

2.9 The effect of NPs on cell viability (cytotoxicity MTT assay)

WI38 lung fibroblast cells (WI001, neuromics, USA) (100 µl/well, 10^5 cells) were incubated until formation of cells' monolayer [45]. RPMI medium was combined with graded concentrations of BV-CS NPs (1000, ……. 31.25 µg/ml) and added to the cells followed by 24 h of incubation. MTT (3-(4,5-dimethylthiazol-2-yl)-2–5-diphenyltetrazolium bromide) with a concentration of 5 mg/ml (20 µl) has been added to the cultures followed by four hours of incubation (37 °C/5% CO_2). To dissolve the formazan that had been developed, dimethylsulfoxide (DMSO) was applied to the cultures and the absorbance was determined at 560 nm.

2.10 Experimental groups

Male Sprague Dawley rats (180–200 g and 10 weeks) were obtained from NODCAR (National Organization for Drug Control and Research, Cairo, Egypt). All experimental procedures were carried out in accordance with the international guidelines for the care and use of laboratory animals and complied with the ARRIVE guidelines. The animals were housed in individual cages in the animal house of NCI at room temperature (20 ± 2 °C) and on 12/12 h light/dark cycle. They were left to acclimatize for a week before the start of the experiment. Animals received standard animal diet (18% crude protein, 5%

crude oil, 54% carbohydrates, vitamins, salts and minerals) and fresh water ad libitum. The sample size was calculated and approved by the ethics committee, where power analysis method was used. The required number of animals in each group have to be < 6 to achieve 80% power with a significance of 0.05. Therefore, twenty-five animals were distributed into five groups (five animals/group):

- Group I: healthy negative control rats,
- Group II: untreated STZ-induced diabetic rats,
- Group III: BV-treated STZ-induced diabetic rats,
- Group IV: unloaded CS-NPs-treated STZ-induced diabetic rats and
- Group V: BV-CS NPs-treated STZ-induced diabetic rats.

Diabetes was brought on by a single intravenous injection (dorsal vein of the penis) of sixty five mg/kg STZ (liquefied in 50 mM Na-citrate buffer to the concentration of 32.5 mg/ml) [46]. FBG was monitored before and after STZ injection (for 7 days), where animals that have FBG level higher than 160 mg/dl were regarded diabetic. Insulin Rat ELISA Kit was used to measure the level of serum insulin concentrations (Invitrogen, ERINS). The average level of glucose in the past three weeks was determined by measuring fructosamine (FTA) by ELISA Kit (MBS2601586, MyBioSource, USA). The treatment dose for BV was 2 mg/kg according to Hassan et al. [18]. BV-CS NPs was dissolved in PBS, where each rat received a volume of NPs solution containing 0.1 mg/kg. Also, unloaded CS NPs was dissolved in PBS and administrated in the same volume as BV-CS NPs. Both of CS NPs and BV-CS NPs were intraperitoneally administrated for 8 weeks after diabetes induction. After the treatment period, rats were anesthetized by 50 mg/kg pentobarbital [47]. Blood was collected by the cardiac puncture method; and serum samples were separated by centrifugation at 1500 rpm for 5 min and then kept at −80 °C. Pancreas from all experimental animals were collected by dissection for preparation of pancreatic homogenates.

2.11 Preparation of pancreatic tissue homogenate

A five ml volume of Tris–HCl buffer with a concentration of 10 mmol and pH of 7.3 was used to homogenize 0.5 g of pancreatic tissue, which was then centrifuged for 10 min at 2000 rpm.

2.12 Biochemical measurements

Triglyceride Assay Kit and Cholesterol Assay Kit (Abcam ab65336 and ab65390) were used to determine the lipid profile levels in the liver and serum. Rat ELISA Kit was used to assess the alanine transaminase (ALT) and aspartate aminotransferase (AST) levels (Abcam ab234579 and MyBioSource MBS264975, respectively). Urea and creatinine levels were estimated by assay kits (Abcam ab285275 and Crystal Chem 80,340, respectively). Measurements of levels of malondialdehyde (MDA), glutathione peroxidase (GPx), and superoxide dismutase (SOD) activities in pancreatic tissue homogenates by rat ELISA Kit were taken to determine the antioxidant capacity of produced BV-CS NPs in vivo (MyBioSource MBS268427, MBS727547 and MBS266897, respectively).

2.13 Immunological measurements

Levels of cytokines (TNF-α, IL-6 and IL-1β) in pancreatic tissue homogenates were evaluated with ELISA kits (Biolegend 438206, MyBioSource MBS355410 and MBS843359, respectively) according to the manufacturer's instruction.

2.14 Statistical analysis

Data were reported as mean ± SD, and examined by one-way analysis of variance (ANOVA) where results with a p value < 0.05 were deemed significant. Because ANOVA provides information, only on the significance between the different groups; it was followed by Bonferroni's post hoc comparisons tests for all statistical analysis. Bonferroni correction is considered a firm post hoc test where it controls the overall type 1 error rate and calculated from: critical value/number of comparisons.

3 Results

3.1 Identification of BV main components

The HPLC chromatogram of BV showed its main components, where melittin, phospholipase A2 and apamin with a retention time of 25.06, 44.50 and 59.4 min, respectively, are noticed in Fig. 1.

3.2 *Encapsulation efficiency (EE) % and* in vitro *release study*

The EE% has been elevated by increasing the concentration of BV. The maximum significant EE% (94.1, 94.2, 94.3, 94.3 and 94.4%) was observed for NPs prepared at BV concentrations of 2, 2.5, 3, 3.5 and 4 mg/ml, respectively (Fig. 2A). Therefore, the selected BV concentration was 2 mg/ml for the preparation of BV-CS NPs. The in vitro release of BV-CS NPs prepared at the optimum conditions (one and half mg/ml chitosan and two mg/ml bee venom) is presented in Fig. 2B. The release profile revealed a sustained release of BV from BV-CS NPs; the release % increased with time to achieve a 98% after 72 h.

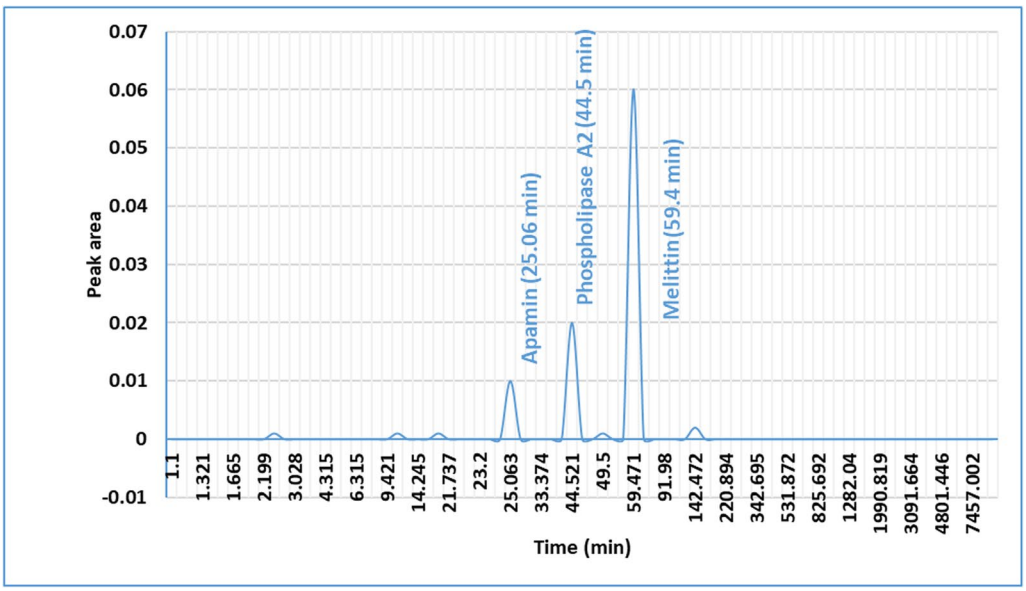

Fig. 1 HPLC chromatogram of bee venom

3.3 Physical characterization of CS NPs and BV-CS NPs

The surface charge (zeta potential) of prepared nanoparticles was 35.4 and 31.2 for CS NPs and BV-CS NPs, respectively (Fig. 2C and D). The shape and surface characteristics of the nanoparticles have been demonstrated using SEM and TEM pictures (Fig. 2E and F), where BV-CS NPs were spherical in form and have a smooth surface. The synthesized BV-CS NPs have a size range of around 80–86 nm. CS NPs and BV-CS NPs had average hydrodynamic sizes of 118.1 nm and 170.2 nm, respectively, as determined by DLS (Fig. 2G). The FTIR spectra of individual free compounds (chitosan and bee venom) and prepared nanoparticles (CS NPs and BV-CS NPs) are presented in Fig. 3. BV spectrum revealed strong peaks at 3410, 1640, 1530, 1239 and 1101 cm^{-1} (Fig. 3B). CS spectra showed two peaks at 3435 and 2923 cm^{-1}, in addition to peaks at 1683 and 1080 cm^{-1} (Fig. 3A). The spectra of CS NPs were different where a wide peak was noticed at 3450 cm^{-1} (Fig. 3C). A peak at 1163 cm^{-1} appeared in the spectra of BV-CS NPs (Fig. 3D).

3.4 Antioxidant activity

The prepared BV-CS NPs have a potential antioxidant activity (DPPH scavenging %), in a dose-dependent style, in comparison with that of ascorbic acid. The antioxidant activities of BV-CS NPs were higher than those of CS NPs at all examined concentrations (Fig. 4A).

3.5 Anti-coagulant activity

The PT and PTT were elevated by increasing the dose of the examined substance (heparin, CS NPs or BV-CS NPs). In comparison with control (heparin), the clotting time of both of CS NPs and BV-CS NPs was significantly lower than that of heparin. The clotting time for both of unloaded CS NPs and BV-CS NPs was nearly the same. The prepared nanoparticles showed a significantly elevated PTT and PT, in a concentration-dependent style (Fig. 4B).

3.6 Anti-inflammatory activity

The prepared BV-CS NPs have significantly ($p < 0.05$) inhibited the RBCs' lysis (Fig. 4C). High percent of hemolysis inhibition (CS NPs: 75.2, 77.2, 81.2, 89.2 and 90.1%; BV-CS NPs: 85.2, 88.2, 90.2, 93.2 and 95.2%) were noticed with increasing concentration from 100 to 800 µg/ml. 1000 µg/ml of CS NPs and BV-CS NPs achieved similar results (94.2 and 98.2%, respectively) to 200 µg/ml indomethacin (99.3%).

3.7 MTT assay

The cytotoxicity % of prepared CS NPs and BV-CS NPs is demonstrated in Fig. 4D. The cytotoxicity % increased with increasing the nanoparticles (CS NPs and BV-CS NPs) concentration. WI38 cells showed a significant viability, after 24 h, with a BV-CS NPs concentration up until 250 µg/ml.

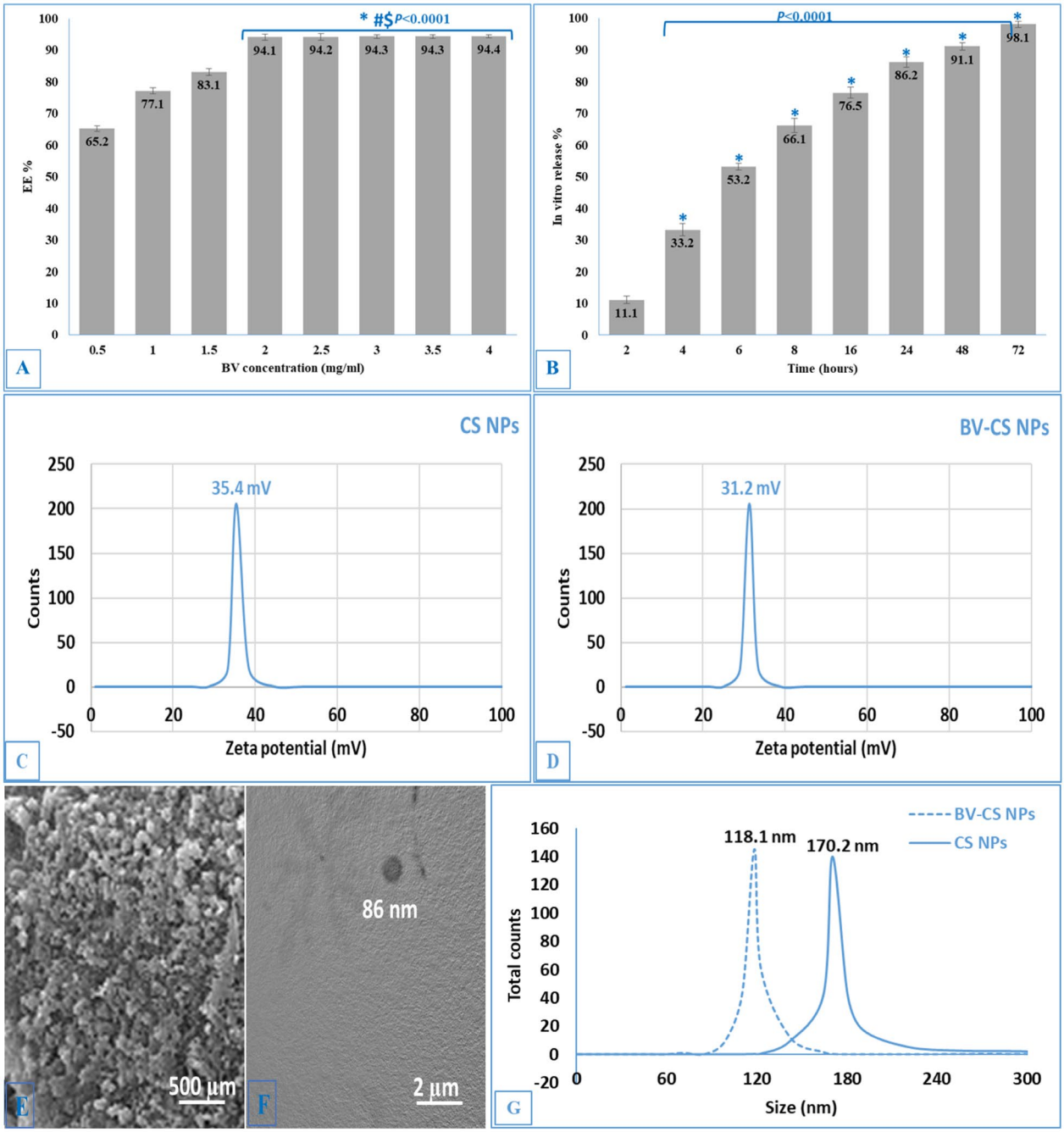

Fig. 2 **A** Encapsulation efficiency (EE%) of BV-CS NPs (chitosan: 1.5 mg/ml and tripolyphosphate: 0.75 mg/ml) (*,# and $ donated significance with regard to BV concentration of 0.5, 1 and 1.5 mg/ml, respectively, at *p* value less than 0.05), **B** percent of BV release from BV-CS NPs in vitro (chitosan: 1.5 mg/ml, tripolyphosphate: 0.75 mg/ml and bee venom: 2 mg/ml) (* donated significance with regard to the release time of 2 h at *p* value less than 0.05), **C** and **D** Zeta potential of CS NPs and BV-CS NPs, respectively, **E** and **F** SEM and TEM image of BV-CS NPs, respectively, **G** size of CS NPs and BV-CS NPs using dynamic light scattering (DLS)

3.8 Biochemical results

Diabetes induction significantly decreased the insulin level (Fig. 5A), in untreated diabetic group, with a significant increase in both of FBG (Fig. 5B) and FTA (Fig. 5C) levels. Administration of BV or unloaded CS NPs led to a significant elevation in the level of insulin and a significant reduction in the levels of FTA and FBG. Conversely, the use of BV-CS NPs in STZ-induced diabetic rats raised

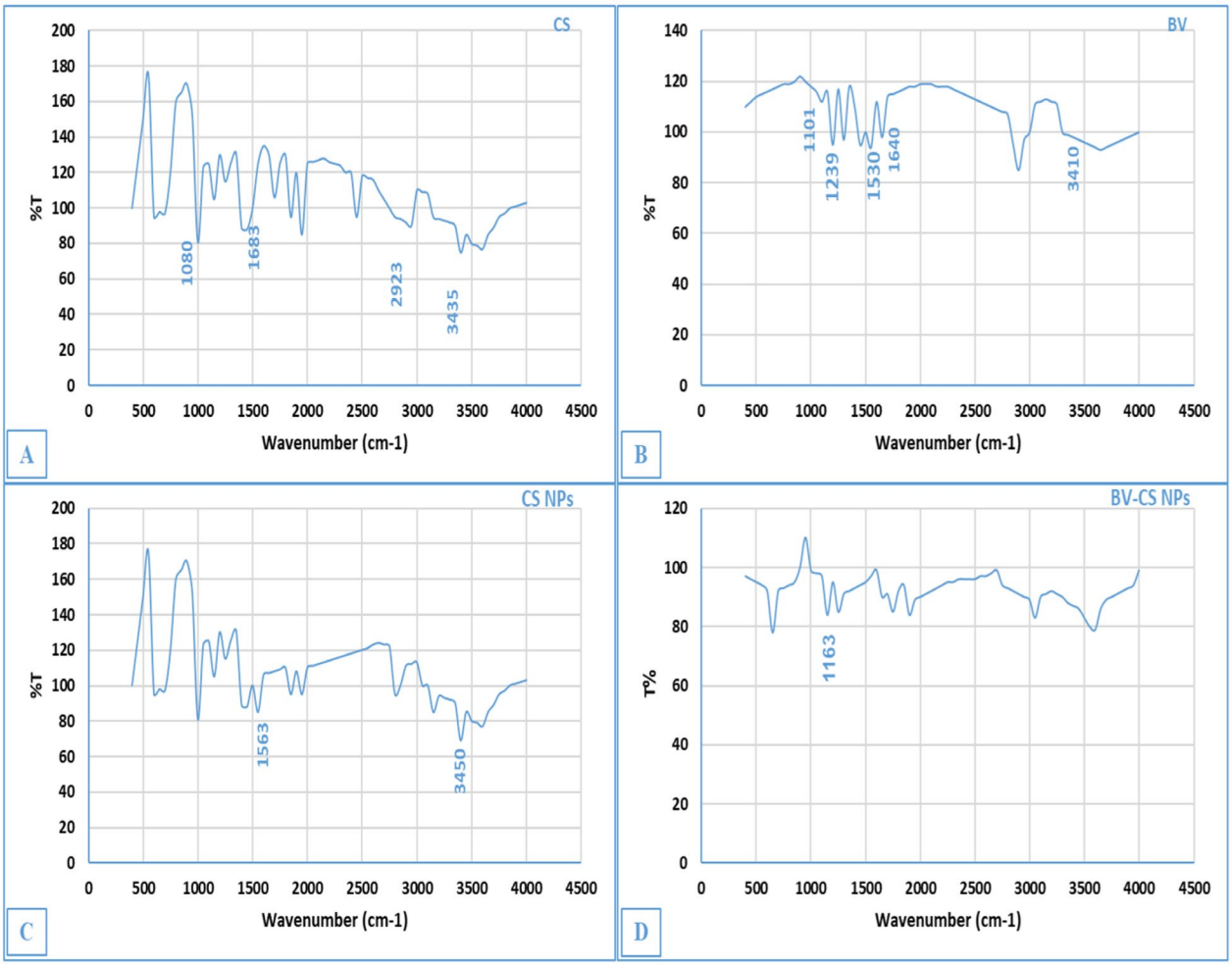

Fig. 3 FTIR spectra of chitosan **A**, bee venom **B**, chitosan nanoparticles **C** and bee venom loaded-chitosan NPs **D**

the insulin levels to a level similar to that of the healthy control group, which resulted in a large drop in the FBG level and, in turn, a considerable drop in the FTA level. Also, diabetes induction decreased body weight in untreated group. The body weights of both BV-CS NPs-treated diabetic group and healthy control group were nearly the same (Fig. 5D).

Untreated diabetic group showed a significant rise in the levels of urea, creatinine (Fig. 6A), ALT and AST (Fig. 6B); in addition to, a disturbance in the lipid profile was obvious in the elevation of triglycerides, cholesterol and low-density lipoprotein (LDL)-C levels (Fig. 6C and D). When comparing the three used treatments, BV-CS NPs administration win the competition as it significantly enhanced the kidney (Fig. 6A) and liver (Fig. 6B) function of treated rats. Moreover, BV-CS NPs administration significantly elevated the high-density lipoprotein (HDL)-C level and reduced the LDL-C level in treated group when compared to diabetic untreated group. Although free BV and unloaded CS NPs significantly ameliorated the serum levels of urea, creatinine, ALT, AST and lipid profile markers in treated groups, their levels remained significantly different from those of healthy control group.

Induction of diabetes by STZ leads to a significant oxidative stress in animals' pancreatic tissue. This was shown by the significant elevation in the MDA level (Fig. 7A) and the significant reduction in the antioxidant enzymes levels (SOD and GPx) (Fig. 7B) in diabetic untreated group. This oxidative stress led to an elevation in the pro-inflammatory cytokines (TNF-α, IL-1β and IL-6) levels (Fig. 7C). Although BV or CS NPs administration reduced the oxidation and inflammation states in treated groups, the best result was observed in BV-CS NPs-treated group. This was obvious in the decrease in MDA and pro-inflammatory cytokine levels and the rise in the antioxidant enzymes levels (SOD and GPx) in BV-CS NPs-treated diabetic group. When comparing the three treated diabetic groups, the highest reduction

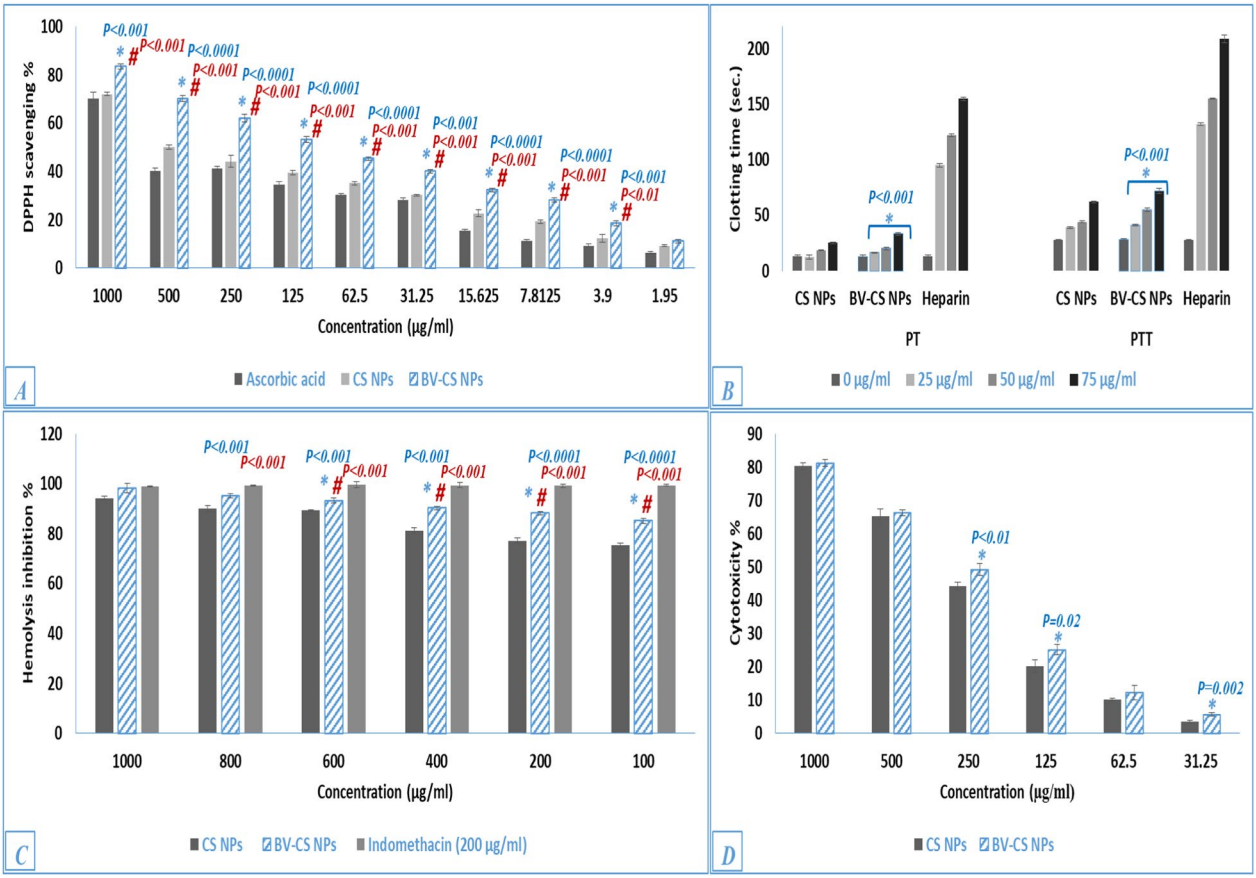

Fig. 4 **A** DPPH scavenging % of CS NPs and BV-CS NPs in comparison with ascorbic acid (* and # donated significance with regard to ascorbic acid and CS NPs, respectively, at *p* value less than 0.05), **B** the anti-coagulant activity of prepared CS NPs and BV-CS NPs (* donates significance with regard to heparin at *p* value less than 0.05), **C** the anti-inflammatory activity of prepared CS NPs and BV-CS NPs (* and # donate significance with regard to indomethacin and CS NPs, respectively, at *p* value less than 0.05) and **D** the cytotoxicity % of prepared CS NPs and BV-CS NPs (* donates significance with regard to CS NPs at *p* value less than 0.05). DPPH: 1, 1-diphenyl-2-picryl hydrazyl

in oxidative stress and inflammation in animals' pancreas was observed in BV-CS NPs-treated diabetic group followed by BV-treated diabetic group and then unloaded CS NPs-treated diabetic group.

4 Discussion

BV may be therapeutically beneficial in controlling the histological and biochemical abnormalities in diabetic rats [22]. Reducing inflammation surrounding pancreatic β cells, possessing antioxidant properties, improving insulin release, and promoting glucose uptake in adipose tissue are possible ways to do this. Khulan et al. [23] examined the hypoglycemic effect of BV in rabbits with alloxan-induced diabetes and reported the decreased inflammation of pancreatic β cells, increased insulin production, and increased absorption of glucose in adipose tissue. BV restored insulin synthesis in a diabetic rat model to normal levels due to its content of phospholipase A2 and melittin polypeptide that enhance insulin secretion [24]. Despite the fact that BV has been shown to provide medical benefits, its safety has remained a major barrier to its acceptance [29]. The adverse reactions to BV ranged from mild skin allergies that go away in a few days to severe, perhaps lethal anaphylactic events. These adverse effects may be explained by an allergic reaction [32], chronic inflammation [33], dosing timings, and BV concentration [29]. The preparation of BV-CS NPs for use as an anti-diabetic medication was the primary goal of the study. Its physical characteristics and effects on oxidation, hemolysis inhibition, coagulation, and cell viability in vitro were then investigated. Rats with STZ-induced diabetes were used to test BV-CS NPs as an anti-diabetic medication. In order to do this, measurements of the animals' body weight, insulin, FTA, and FBG levels in the experimental groups were made. In vivo, pancreatic tissue homogenates were used to assess the impact of BV-CS NPs on the decrease of oxidation and inflammation.

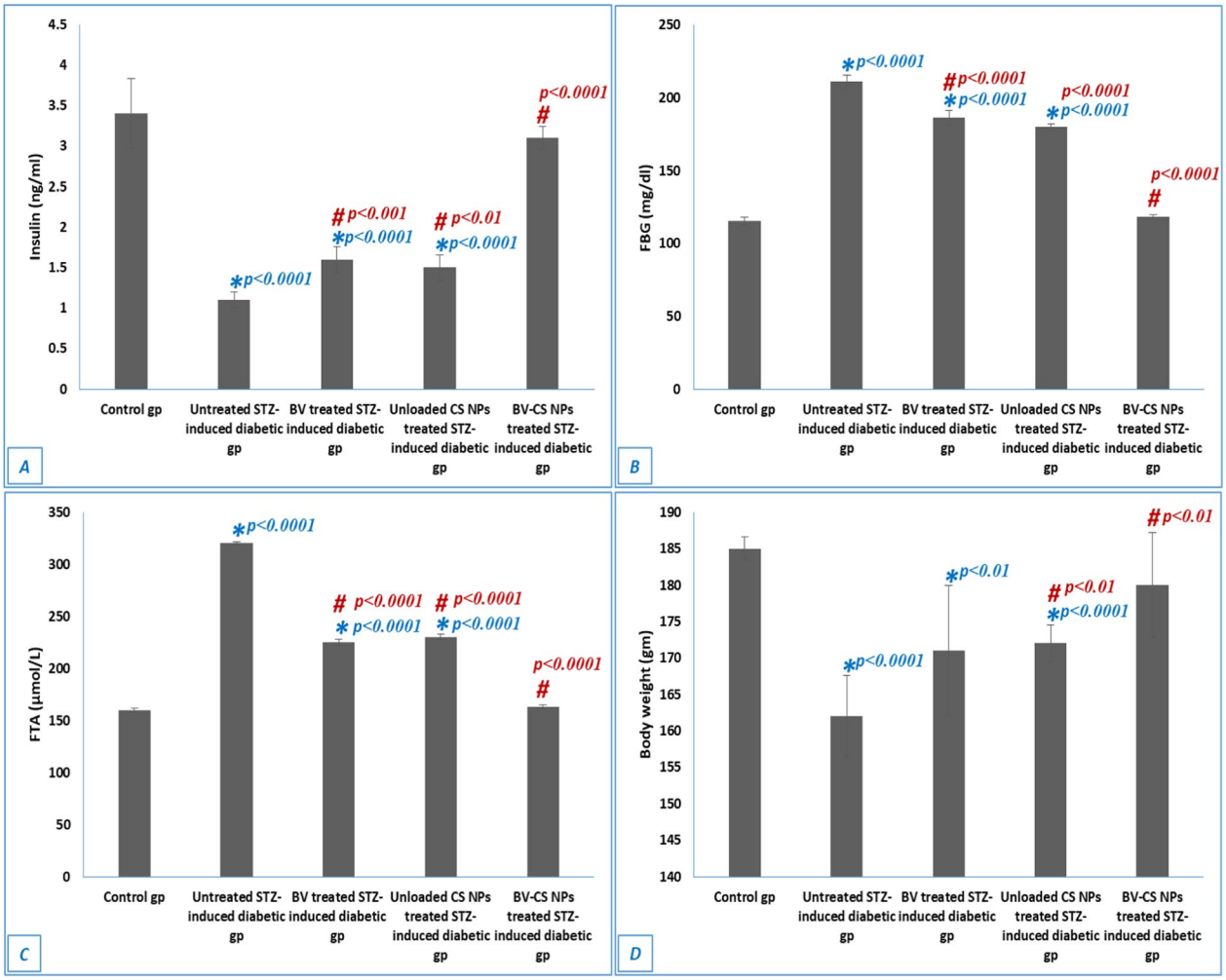

Fig. 5 Level of **A** insulin, **B** FBG, **C** FTA and **D** body weight in different experimental groups, where *represents significance compared with the healthy control group and #represents significance compared with the untreated STZ-diabetic group ($P < 0.05$). FBG: fasting blood glucose and FTA: fructosamine

According to our results, CS NPs that were loaded with a minimal concentration of BV (2 mg/mL) were chosen for more characterization and application (based on the EE% results). CS NPs and BV-CS NPs were made and examined at various magnifications using SEM and TEM. The bulk of the NPs seemed to have smooth surfaces, a homogenous distribution, and a spherical shape. Moreover, the surface charge of CS NPs and BV-CS NPs was 35.4 and 31.2, respectively. This decrease in zeta potential indicated the stability of prepared BV-CS NPs; and the importance of TPP as a cross-linking agent. In addition, our results demonstrated that the ionic gelation method created a stable nanoparticles and protected BV-CS NPs from agglomeration.

Our results showed a significant positive relationship between BV concentrations and EE%; it was caused by reactions between chitosan and bee venom and the cross-linking of chitosan with triphosphate/bee venom. Studies on the impact of protein content on EE% have produced conflicting and inconclusive results [48]. Our results were in agreement with those of Avadi et al. [49] and Mohammadpourdounighi et al. [50], but it was opposite to that of Xu and Du [51], who agreed on bovine serum albumin (BSA) encapsulation. The similar pattern was, also, observed by Sabnis and Block [52] and Somnuk et al. [53] for ribonuclease A, alpha-Lactalbumin and cytochrome C. Moreover, the release pattern of bee venom from nanoparticles showed a burst release ˃50% after 6 h. The breakdown of BV molecules that were weakly attached to the surface of the CS NPs caused this rapid burst action in the first six hours [54]. The BV was quickly released in the first few hours due to the NPs' large specific surfaces, and thereafter the gradual

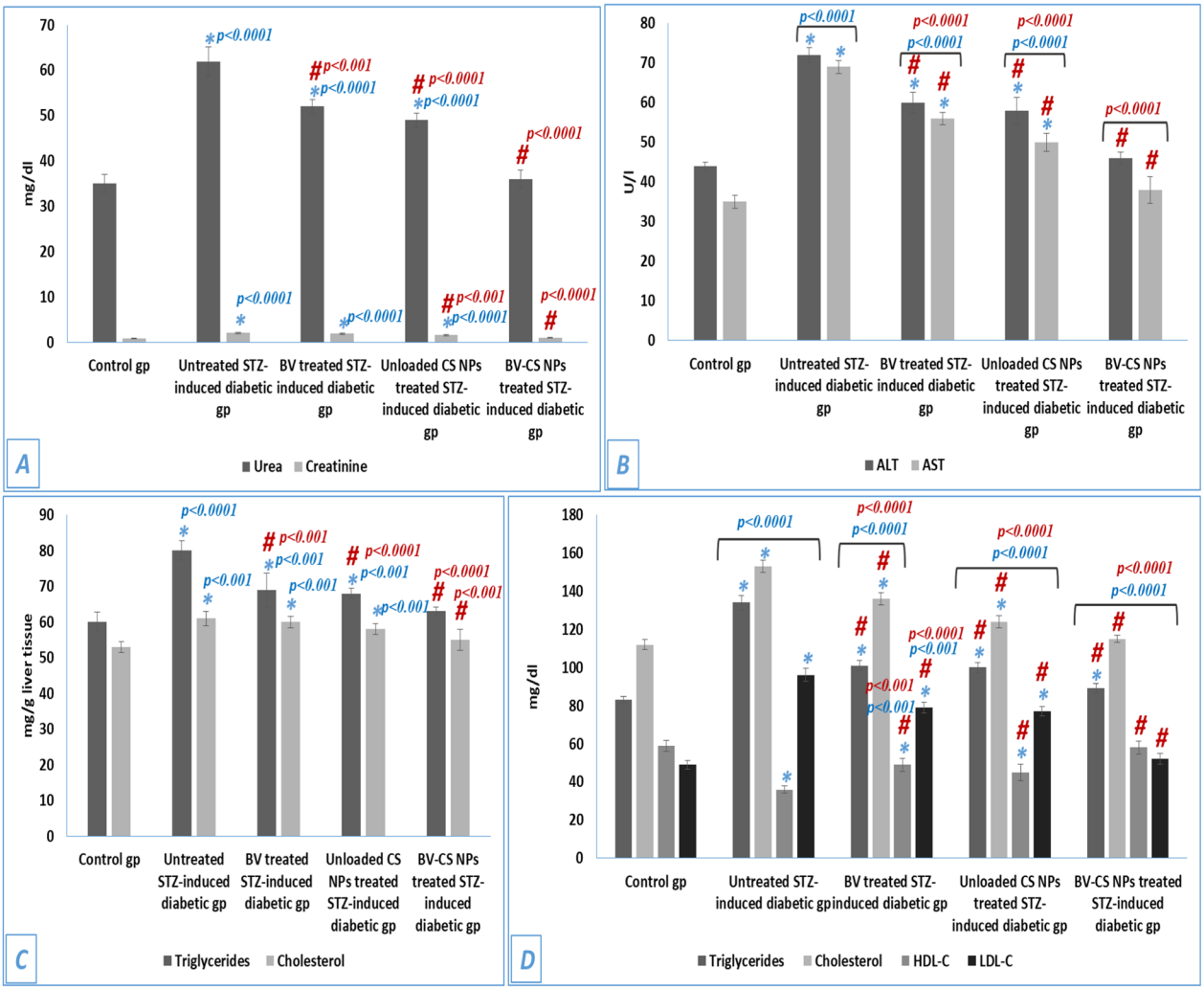

Fig. 6 Level of **A** kidney function parameters (urea and creatinine), **B** liver function enzymes (ALT and AST), **C** and **D** lipid profile (triglycerides, cholesterol, HDL-C and LDL-C) in liver tissue and serum, where *represents significance compared with the healthy control group and #represents significance compared with the untreated STZ-diabetic group ($P < 0.05$). ALT: alanine transaminase, AST: aspartate aminotransferase, HDL-C: high-density lipoprotein-cholesterol and LDL-C: low-density lipoprotein-cholesterol

disintegration of the nanoparticles caused the release of the entrapped BV at a stable rate [48].

The efficacy of the ionic gelation process to produce NPs was assessed using FTIR. The N–H stretching free vibrations were indicated by the measured peak in the BV spectrum's absorbance range of 3245–3454 cm^{-1}. The FTIR spectrum of BV also indicated the characteristic amide bands at 1640 cm^{-1} and 1530 cm^{-1} for amide I and II, respectively. Moreover, bands identified at 1101 cm^{-1} and 1239 cm^{-1} suggested the unsystematic coil shape. The noticeable peak in the chitosan spectra's 3290–3450 cm^{-1} area was due to the combined peaks of intermolecular hydrogen bonding and O–H stretching. The NH originating from primary amines overlapped in the same region. A peak at 1080 cm^{-1} in the amide I band of the secondary amide's carbonyl (C=O] stretching absorption spectrum corresponds to the C–O–C bond stretching. CS NPs and BV-CS NPs have distinct spectra. In CS NPs, the peak at 3450 cm^{-1} broadened and the relative intensity increased, indicating improved hydrogen bonding. The 1683 cm^{-1} peak of the NH_2 bending vibration was, also, modified to 1563 cm^{-1}. The cross linkage with TPP was further shown by an assigned P=O peak on the cross-linked chitosan at 1163 cm^{-1}. According to Saber et al. [55], the peak corresponding to the bending vibration of N–H bond in CS NPs was moved (1633–1562 cm^{-1}) and a sharp new peak was developed (1642 cm^{-1}). The CS saccharide structure was indicated

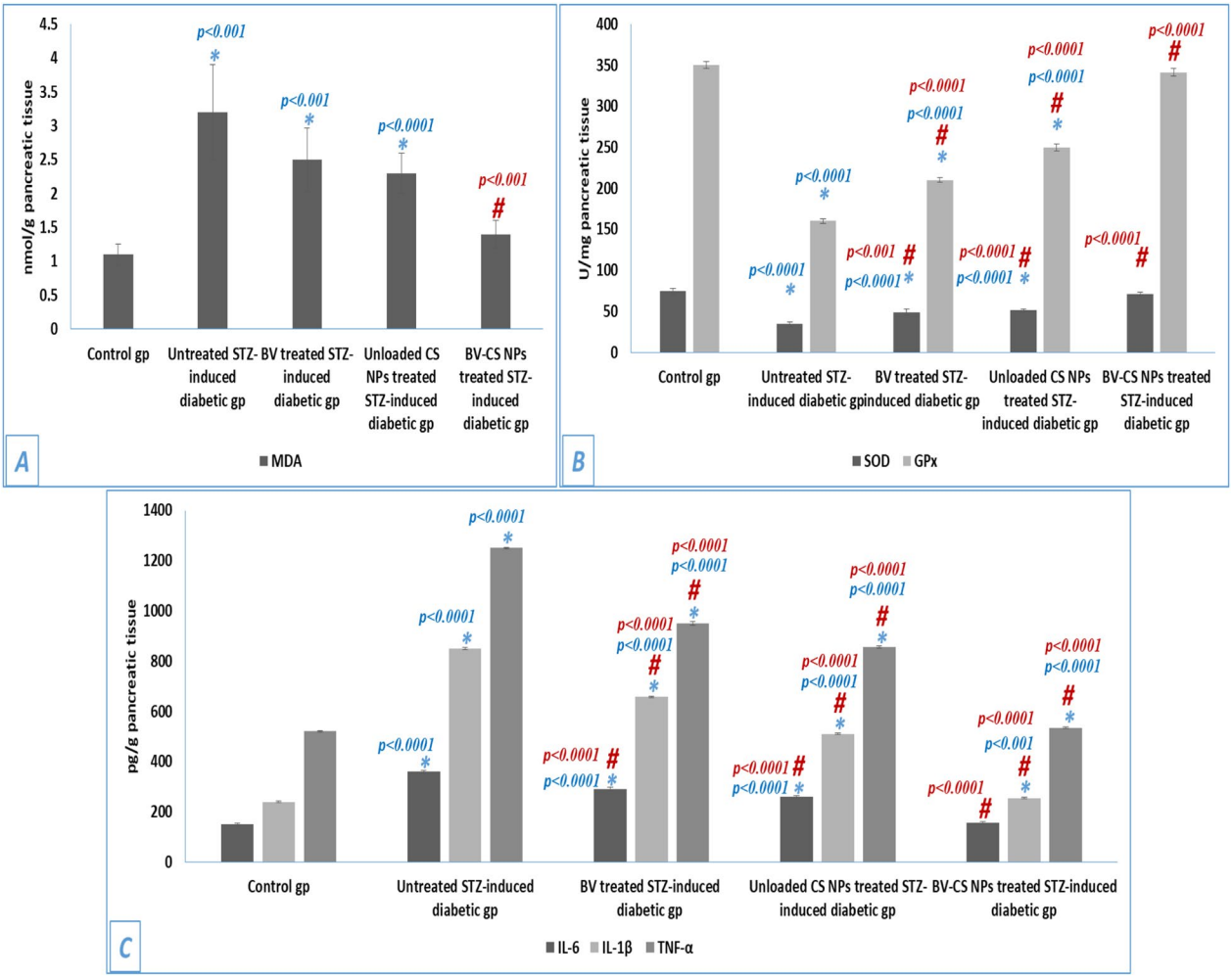

Fig. 7 level of **A** and **B** oxidative stress markers (MDA, SOD, and GPx) and **C** pro-inflammatory cytokines (IL-6, IL-1β and TNF-α) in pancreatic tissue homogenates. where *represents significance compared with the healthy control group and # represents significance compared with the untreated STZ-diabetic group ($P < 0.05$). MDA: malondialdehyde, SOD: superoxide dismutase, GPx: glutathione peroxides, IL: interleukin and TNF: tumor necrosis factor

by the peak at 894 cm^{-1} [56]. Moreover, since the FTIR spectrum agreed with the outcome of the CS film's phosphate modification, it is assumed that phosphoric and ammonium ions interacted to produce the observed results [57]. Consequently, in NPs, the PO_4^{3-} group of tripolyphosphate was connected with the $-NH_2$ group of chitosan [58].

Three peaks are identified by Sharma and Sharma [58] as defining characteristics of CS: the broad and strong hydrogen-bonding stretching O–H peak at 3500–3300 cm^{-1}; the $-NH_2$ peak at approximately 1633 cm^{-1}; and the asymmetrically stretching C–O–C peak at approximately 1150 cm^{-1} [48]. The relative strength of the signal at 3450 cm^{-1} rose in CS NPs, showing that the hydrogen bonding has been improved. The attachment and encapsulation of bee venom (anionic protein molecules) with chitosan molecules (cationic) are challenging due to the 3D conformation and solution condition. This is attributed to the 3D folded protein nature of bee venom which is impacted by various solution limitations. In addition to serving as a cross-linker, TPP also creates additional H-bonds with the $-NH_2$ groups on the chitosan and bee venom molecules leading to tightly packed BV-CS NPs. More BV molecule adsorption on the surface of newly produced CS NPs may take place sequentially, increasing the amount of protein loaded onto the particles [44].

In this work, we assessed the produced BV-CS NPs' in vitro antioxidant, hemolysis inhibition, anti-coagulant, and cytotoxicity effects before using them in vivo.

The findings suggested that BV-CS NPs can be utilized as an effective treatment for diabetes in a safe manner. The produced BV-CS NPs showed potential antioxidant, membrane stabilizing, and non-cytotoxic properties up to a concentration of 250 µg/ml. Our results showed that free BV and unloaded CS NPs administration slightly managed blood glucose level and metabolic abnormalities that followed diabetes induction. However, on comparing BV-CS NPs-treated diabetic group with free BV or unloaded CS NPs-treated diabetic groups; we found that BV-CS NPs won the competition. The prepared BV-CS NPs showed a hypoglycemic effect in STZ-induced diabetic rats; as it reduced FBG and FTA levels. Moreover, it reduced the increase in the liver and kidney function parameters that results from diabetes induction. The oxidative stress and inflammation in animal's pancreas were evaluated to determine the antioxidant and anti-inflammatory effects of BV-CS NPs in vivo. This was done by measuring the lipid peroxidation marker (MDA) and the antioxidant enzymes (SOD and GPx); in addition to the pro-inflammatory cytokines (IL1β, IL-6 and TNF-α). The overabundance of reactive oxygen species (ROS) in tissues and cells that cannot be removed by the antioxidant system is known as oxidative stress. An imbalance in this defense system can lead to damage to biological components such as proteins, lipids, and DNA [59]. An increase in free radicals leads to an excess production of MDA. The amount of MDA in a patient is a typical measure of oxidative stress and their antioxidant status [60]. IL-1β is an influential pro-inflammatory cytokine that is essential for organism-defense toward injuries and/or diseases [61]. The soluble mediator IL-6 affects inflammation, immunological response, and hematopoiesis in a pleiotropic manner. Furthermore, IL-6 plays a pivotal role in the integration of innate and acquired immune responses by promoting the unique development of naïve CD4 + T cells. When inflammation is acute, macrophages and monocytes release a cytokine called TNF-α. It sets off a number of signaling pathways in cells that may lead to apoptosis or necrosis [62, 63]. The study showed that BV-CS NPs, also, reduced the oxidative stress and increased the antioxidant defense system and decreased the inflammatory markers in pancreatic tissue homogenates in treated group. BV-CS NPs showed a hypolipidemic effect and increased insulin secretion in treated rats.

These results can be explained by the combined beneficial medicinal properties of BV and CS, where both have antioxidant and anti-inflammatory effects. BV contains major bioactive components (melittin and phospholipase A2) that accounts to its hypoglycemic effects. Therefore, BV-CS NPs stimulated insulin secretion and increased the uptake of glucose and lipid into adipose tissue. Our results were in similar to those of Mousavi et al. [24], who confirmed that BV has hypoglycemia and hypolipidemic effects in diabetic animals. Khulan et al. [23] showed that melittin and phospholipase A2, a polypeptide and an enzyme that together account up to 62% of the BV, were responsible for these effects. By the direct stimulation of insulin production and the prevention of β cell inflammation, BV reduced blood glucose levels [64]. Melittin starts a process of membrane depolarization that, depending on the level of extracellular calcium, increases the amount of calcium ions that enter β cells through calcium channels leading to insulin secretion [23]. Increasing insulin activity in fat cells, which results in decreased LDL, triglyceride, and higher HDL levels, is another potential treatment option for diabetic dyslipidemia [65]. Phospholipase A2 in BV partly lyses cell membrane by acting enzymatically on plasmatic lipoproteins [66]. Via partial adipocyte membrane lyses and binding of more insulin molecules, this action promotes glucose and lipid uptake into adipose tissue. According to certain investigations, phospholipase A2 from BV is more likely to bind to plasmatic lipoproteins and induce cytotoxicity by producing free fatty acids and lysophospholipids, esterifying free cholesterol in HDL in the process [67].

In conclusion, the prepared nanoparticles enabled us to use small dose of BV and achieved a controlled sustainable release. BV-CS NPs decreased blood glucose level and increased insulin level. It reduced oxidative stress by decreasing MDA level and increasing the antioxidant enzymes (SOD and GPx) levels and decreased the pro-inflammatory cytokines (IL-6, IL-1β and TNF-α) levels. The prepared BV-CS NPs was safe to be used in vivo and succeeded as an anti-diabetic therapy in rat model. To our knowledge, this is the first work to use BV-CS NPs for treatment of diabetes; the study can be a new hope for treatment of diabetic patients. The study has some limitations such as the testing of a single dose of BV-CS NPs and small number of animals. We recommend the test of different doses of BV-CS NPs in diabetic animal models and examine their effects on pancreatic β cells neogenesis.

Abbreviations

ALT	Alanine transaminase
AST	Aspartate aminotransferase
BV	Bee venom
BV-CS NPs	Bee venom loaded-chitosan nanoparticles
C	Cholesterol
CS	Chitosan
DM	Diabetes mellitus
DMSO	Dimethylsulfoxide
DPPH	1, 1-Diphenyl-2-picryl hydrazyl
EE	Encapsulation efficiency
FBG	Fasting blood glucose
FTA	Fructosamine
FTIR	Fourier transform infrared

GPx	Glutathione peroxidase
H&E	Hematoxylin and eosin
HDL	High-density lipoprotein
HPLC	High-performance liquid chromatography
i.p	Intraperitoneal
IL	Interleukin
LDL	Low-density lipoprotein
MDA	Malondialdehyde
MTT	3-(4,5-Dimethylthiazol-2-yl)-2–5-diphenyltetrazolium bromide
NF-κB	Nuclear factor-κB
NODCAR	National organization for drug control and research
NPs	Nanoparticles
PDI	Polydispersity index
PT	Prothrombin time
PTT	Partial thromboplastin time
SOD	Superoxide dismutase
STZ	Streptozotocin
TEM	Transmission electron microscope
TNF	Tumor necrosis factor
TPP	Sodium tripolyphosphate

Acknowledgements
Not applicable.

Author contributions
A.F. and G.S. were involved in the conceptualization, methodology and writing the manuscript. A.M., A.A. and F.M. contributed to the data curation, methodology, visualization and investigation. A.F. and G.S. contributed to software and validation. All authors have read and approved the manuscript.

Funding
This research did not receive any specific grant from funding agencies in the public, commercial, or not-for-profit sectors.

Availability of data and materials
The data will be made available on reasonable request from the corresponding author.

Declarations

Ethical approval and consent to participate
All experimental procedures were carried out in accordance with the international guidelines for the care and use of laboratory animals and complied with the ARRIVE guidelines and were approved by the Institutional Animal Care and Use Committee (2023) of October University for Modern Sciences and Arts. The study was conducted in accordance with the guide for the care and use of laboratory animals, Eighth edition (2011).

Consent for publication
Not applicable.

Competing interests
The authors declare that they have no competing interests.

Author details
[1]Biotechnology Department, Faculty of Science, Cairo University, Giza, Egypt. [2]Faculty of Biotechnology, October University for Modern Sciences and Arts (MSA), Giza, Egypt.

Received: 6 June 2024 Accepted: 15 September 2024
Published online: 30 September 2024

References

1. Tan SY, Mei Wong JL, Sim YJ, Wong SS, Mohamed Elhassan SA, Tan SH, Ling Lim GP, Rong Tay NW, Annan NC, Bhattamisra SK, Candasamy M (2019) Type 1 and 2 diabetes mellitus: a review on current treatment approach and gene therapy as potential intervention. Diabetes Metab Syndr 13(1):364–372
2. Forouhi NG, Wareham NJ (2014) Epidemiol Diabetes Med (Abingdon) 42(12):698–702
3. English E, Lenters-Westra E (2018) HbA1c method performance: the great success story of global standardization. Crit Rev Clin Lab Sci 55(6):408–419
4. Abdulah DM, Hassan AB, Saadi FS, Mohammed AH (2018) Impacts of self-management education on glycaemic control in patients with type 2 diabetes mellitus. Diabetes Metab Syndr 12(6):969–975
5. Quianzon CC, Cheikh IE (2012) History of current non-insulin medications for diabetes mellitus. J Commun Hosp Intern Med Perspect 2(3):19081
6. Chaudhury A, Duvoor C, Reddy Dendi VS, Kraleti S, Chada A, Ravilla R, Marco A, Shekhawat NS, Montales MT, Kuriakose K, Sasapu A, Beebe A, Patil N, Musham CK, Lohani GP, Mirza W (2017) Clinical review of antidiabetic drugs: implications for type 2 diabetes mellitus management. Front Endocrinol (Lausanne) 8:6
7. Thakare V, Shende SS, Shirure PA, Swami OC (2017) Role of conventional oral antidiabetic drugs in management of type 2 diabetes mellitus. IJRMS 5:749–758
8. Hossen MS, Gan SH (2017) Khalil MI (2017) Melittin, a potential natural toxin of crude bee venom: probable future arsenal in the treatment of diabetes mellitus. J Chem 2:1–7
9. Zhu Y, Zhao J, Luo L, Gao Y, Bao H, Li P, Zhang H (2021) Research progress of indole compounds with potential antidiabetic activity. Eur J Med Chem 223:113665
10. Hassan SM, Farid A, Panda SS, Bekheit MS, Dinkins H, Fayad W, Girgis AS (2024) Indole compounds in oncology: therapeutic potential and mechanistic insights. Pharmaceuticals (Basel) 17(7):922
11. Kim SH, Yum HW, Kim SH, Kim W, Kim SJ, Kim C, Kim K, Suh YG, Surh YJ (2021) Protective effects of taurine chloramine on experimentally induced colitis: NFκB, STAT3, and Nrf2 as potential targets. Antioxidants (Basel) 10(3):479
12. Hekmatpou D, Mehrabi F, Rahzani K, Aminiyan A (2019) The effect of aloe vera clinical trials on prevention and healing of skin wound: a systematic review. Iran J Med Sci 44(1):1–9
13. Roudbari L, Imani S (2012) The effects of Androctonus crassicauda scorpion venom in the treatment of diabetes mellitus type 1 in animal models. Ann Biol Res 3:5782–5785
14. Khalil A, Elesawy BH, Ali TM, Ahmed OM (2021) Bee venom: from venom to drug. Molecules 26(16):4941
15. Wehbe R, Frangieh J, Rima M, El Obeid D, Sabatier JM, Fajloun Z (2019) Bee venom: overview of main compounds and bioactivities for therapeutic interests. Molecules 24(16):2997
16. Im EJ, Kim SJ, Hong SB, Park JK, Rhee MH (2016) Anti-Inflammatory activity of bee venom in BV2 microglial cells: mediation of MyD88-dependent NF-κB signaling pathway. Evid Based Complement Alternat Med 2016:3704764
17. Ahmed O, Fahim H, Mahmoud A, Eman Ahmed EA (2017) Bee venom and hesperidin effectively mitigate complete freund's adjuvant-induced arthritis via immunomodulation and enhancement of antioxidant defense system. Arch Rheumatol 33(2):198–212
18. Carpena M, Nuñez-Estevez B, Soria-Lopez A, Simal-Gandara J (2020) Bee Venom: an updating review of its bioactive molecules and its health applications. Nutrients 12(11):3360
19. Hassan SA, Alazragi RS, Salem NA (2021) Potential therapeutic effect of bee venom on cisplatin-induced hepatotoxicity. J Pharm Res Int 33:200–210
20. Cornara L, Biagi M, Xiao J, Burlando B (2017) Therapeutic properties of bioactive compounds from different honeybee products. Front Pharmacol 8:412
21. Oršoli´c N, (2012) Bee venom in cancer therapy. Cancer Metastasis Rev 31:173–194
22. Hassan AK, El-kotby DA, Tawfik MM, Badr RE, Bahgat IM (2019) Antidiabetic effect of the Egyptian honey bee (Apis mellifera) venom in alloxan-induced diabetic rats. JoBAZ 80:58
23. Khulan TS, Ambaga M, Chimedragcha CH (2015) Effect of honeybee venom (Apis mellifera) on hyperglycemia and hyperlipidemia in alloxan induced diabetic rabbits. J Diabetes Metab 6:507
24. Mousavi SM, Imani S, Haghighi S, Mousavi SE, Karimi A (2012) Effect of Iranian honey bee (apis mellifera) venom on blood glucose and insulin in diabetic rats. J Arthropod Borne Dis 6(2):136–143

25. Sattar A-S (2022) Metformin and bee venom enhanced histological changes of the pancreas in diabetic mice. Wasit J Pure Sci 1:192–201
26. Zahran F, Mohamed A, Zein N (2021) Bee venom attenuates degenerative effects of diabetes associated with hyperlipidemia in rats. Biochem Lett 17:77–107
27. Ullah A, Aldakheel FM, Anjum SI, Raza G, Khan SA, Tlak Gajger I (2023) Pharmacological properties and therapeutic potential of honey bee venom. Saudi Pharm J 31(1):96–109
28. Simonsson E, Karlsson S, Ahrén B (2000) Islet phospholipase A(2) activation is potentiated in insulin resistant mice. Biochem Biophys Res Commun 272(2):539–543
29. Zhang S, Liu Y, Ye Y, Wang XR, Lin LT, Xiao LY, Zhou P, Shi GX, Liu CZ (2018) Bee venom therapy: potential mechanisms and therapeutic applications. Toxicon 148:64–73
30. Park JH, Yim BK, Lee JH, Lee S, Kim TH (2015) Risk associated with bee venom therapy: a systematic review and meta-analysis. PLoS ONE 10(5):e0126971
31. Cherniack EP, Govorushko S (2018) To bee or not to bee: The potential efficacy and safety of bee venom acupuncture in humans. Toxicon 154:74–78
32. Bilò BM, Bonifazi F (2011) Hymenoptera venom immunotherapy. Immunotherapy 3(2):229–246
33. Yoo J, Lee G (2022) Adverse events associated with the clinical use of bee venom: a review. Toxins (Basel) 14(8):562
34. Chen J, Lariviere WR (2010) The nociceptive and anti-nociceptive effects of bee venom injection and therapy: a double-edged sword. Prog Neurobiol 92(2):151–183
35. Chen J, Guan SM, Sun W, Fu H (2016) Melittin, the major pain-producing substance of bee venom. Neurosci Bull 32(3):265–272
36. Xing L, Dawei C, Liping X, Rongqing Z (2003) Oral colon-specific drug delivery for bee venom peptide: development of a coated calcium alginate gel beads-entrapped liposome. J Control Release 93(3):293–300
37. Nasser M, Abd El-atif MB, Alaa H, Abdelaziz M, Mustafa M, Masour M, Magdy S, Mohsen S, El-karamany Y, Farid A (2024) Discovering the antiparasitic activity of melatonin loaded lecithin/chitosan nanoparticles against giardiasis and cryptosporidiosis in Balb/c infected mice. Beni-Suef Univ J Basic Appl Sci
38. Madbouly N, Ooda A, Nabil A, Nasser A, Ahmed E, Ali F, Mohamed F, Faried H, Badran M, Ahmed M, Ibrahim M, Rasmy M, Saleeb M, Riad V, Ibrahim Y, Farid A (2024) The renoprotective activity of amikacin-gamma-amino butyric acid-chitosan nanoparticles: a comparative study. Inflammopharmacology. https://doi.org/10.1007/s10787-024-01464-5
39. Mohammed MA, Syeda JTM, Wasan KM, Wasan EK (2017) An overview of chitosan nanoparticles and its application in non-parenteral drug delivery. Pharmaceutics 9(4):53
40. Rezaei Mokarram A, Alonso MJ (2006) Preparation and evaluation of chitosan nanoparticles containing Diphtheria toxoid as new carriers for nasal vaccine delivery mice. Arch Razi Inst 61:13–25
41. Ralston K, Petri W (2011) Tissue destruction and invasion by Entamoeba histoltica. Trends Parasitol 27:253–262
42. Elnosary ME, Aboelmagd HA, Habaka MA, Salem SR, El-Naggar ME (2023) Synthesis of bee venom loaded chitosan nanoparticles for anti-MERS-COV and multi-drug resistance bacteria. Int J Biol Macromol 224:871–880
43. Kruger NJ (1994) The Bradford method for protein quantitation. Methods Mol Biol 32:9–15
44. Gan Q, Wang T, Cochrane C, McCarron P (2005) Modulation of surface charge, particle size and morphological properties of chitosan-TPP nanoparticles intended for gene delivery. Coll Surf B Biointerfaces 44(2–3):65–73
45. Farid A, Ahmed A, Alaa O, Safwat G (2024) Desert date seed extract-loaded chitosan nanoparticles ameliorate hyperglycemia and insulin deficiency through the reduction in oxidative stress and inflammation. Sci Rep 14(1):5829
46. Furman BL (2015) Streptozotocin-induced diabetic models in mice and rats. Curr Protoc Pharm 70:5.47.1-5.47.20
47. Mohamed AS, Hosney M, Bassiony H, Hassanein SS, Soliman AM, Fahmy SR, Gaafar K (2020) Sodium pentobarbital dosages for exsanguination affect biochemical, molecular and histological measurements in rats. Sci Rep 10:378
48. Zolfagharian H, Damavandi M, Mohammadpour Dounighi N, Moradi S (2012) Preparing and characterizing chitosan nanoparticles containing Hemiscorpius lepturus scorpion venom as an antigen delivery system. Arch Razi Inst 67:145–153
49. Avadi MR, Sadeghi AM, Mohammadpour N, Abedin S, Atyabi F, Dinarvand R, Rafiee-Tehrani M (2010) Preparation and characterization of insulin nanoparticles using chitosan and Arabic gum with ionic gelation method. Nanomedicine 6(1):58–63
50. Mohammadpourdounighi N, Behfar A, Ezabadi A, Zolfagharian H, Heydari M (2010) Preparation of chitosan nanoparticles containing Naja naja oxiana snake venom. Nanomedicine 6(1):137–143
51. Xu Y, Du Y (2003) Effect of molecular structure of chitosan on protein delivery properties of chitosan nanoparticles. Int J Pharm 250(1):215–226
52. Sabnis S, Block LH (2000) Chitosan as an enabling excipient for drug delivery systems. I Molecular modifications. Int J Biol Macromol 27(3):181–186
53. Somnuk J, Anupap T, Virote B (2011) Preparation of chitosan nanoparticles for encapsulation and release of protein. Korean J Chem Eng 28:1247–1251
54. Amidi M, Romeijn SG, Borchard G, Junginger HE, Hennink WE, Jiskoot W (2006) Preparation and characterization of protein-loaded N-trimethyl chitosan nanoparticles as nasal delivery system. J Control Release 111(1–2):107–116
55. Saber AE, Abdelwahab AK, el Amir AM, Nassar MI, Zohdi HF (2017) Bee venom loaded chitosan nanoparticles as treatment for amoebiasis in mice. J Egypt Soc Parasitol 47(2):443–58
56. Silverstein RM, Webster FX, Kiemle D (2005) Spectrometric identification of organic compounds, 7th edn. Wiley, New York
57. Mikušová V, Mikuš P (2021) Advances in chitosan-based nanoparticles for drug delivery. Int J Mol Sci 22(17):9652
58. Sharma S, Sharma U (2013) Synthesis, characterisation and determination of encapsulation efficiency of chitosan nanoparticles for terbinafine. Indo Am J Pharm Res 3:1564–1567
59. Ďuračková Z (2010) Some current insights into oxidative stress. Physiol Res 59(4):459–469
60. Gaweł S, Wardas M, Niedworok E, Wardas P (2004) Dialdehyd malonowy (MDA) jako wskaźnik procesów peroksydacji lipidów w organizmie [Malondialdehyde (MDA) as a lipid peroxidation marker]. Wiad Lek 57(9–10):453–455
61. Lopez-Castejon G, Brough D (2011) Understanding the mechanism of IL-1β secretion. Cytokine Growth Factor Rev 22(4):189–195
62. Idriss HT, Naismith JH (2000) TNF alpha and the TNF receptor superfamily: structure–function relationship(s). Microsc Res Tech 50(3):184–195
63. Amr M, Farid A (2024) Impact of cow, buffalo, goat or camel milk consumption on oxidative stress, inflammation and immune response post weaning time. Sci Rep 14(1):9967
64. Park HJ, Lee HJ, Choi MS, Son DJ, Song HS, Song MJ, Lee JM, Han SB, Kim Y, Hong JT (2008) JNK pathway is involved in the inhibition of inflammatory target gene expression and NF-kappaB activation by melittin. J Inflamm 5:7
65. Ide S, Maezawa Y, Yokote K (2023) Updates on dyslipidemia in patients with diabetes. J Diabetes Investig 14(9):1041–1044
66. Singh J, Ranganathan R (2012) Quantitation of lysolipids, fatty acids, and phospholipase A2 activity and correlation with membrane polarity. J Lipid Res 53(9):1993–2001
67. Guillaume C, Calzada C, Lagarde M, Schrével J, Deregnaucourt C (2006) Interplay between lipoproteins and bee venom phospholipase A2 in relation to their anti-Plasmodium toxicity. J Lipid Res 47(7):1493–1506

Publisher's Note